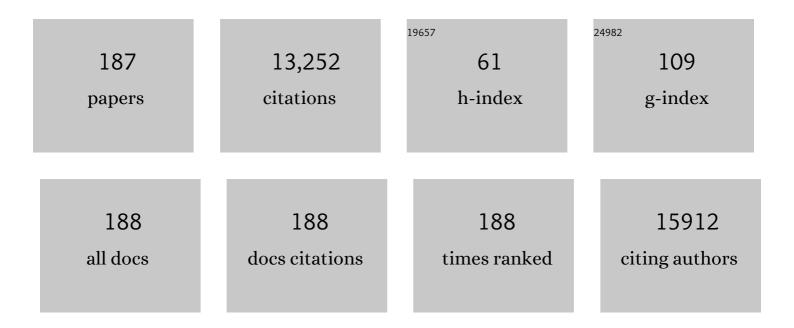
List of Publications by Year in descending order

Source: https://exaly.com/author-pdf/1639930/publications.pdf Version: 2024-02-01



#	Article	IF	CITATIONS
1	Hydrophilic Cu <sub>9</sub> S <sub>5</sub> Nanocrystals: A Photothermal Agent with a 25.7% Heat Conversion Efficiency for Photothermal Ablation of Cancer Cells <i>in Vivo</i> . ACS Nano, 2011, 5, 9761-9771.	14.6	1,155
2	Hydrophilic Flowerâ€Like CuS Superstructures as an Efficient 980 nm Laserâ€Driven Photothermal Agent for Ablation of Cancer Cells. Advanced Materials, 2011, 23, 3542-3547.	21.0	760
3	Sub-10 nm Fe <sub>3</sub> O <sub>4</sub> @Cu <sub>2–<i>x</i></sub> S Core–Shell Nanoparticles for Dual-Modal Imaging and Photothermal Therapy. Journal of the American Chemical Society, 2013, 135, 8571-8577.	13.7	581
4	Ultrathin PEGylated W <sub>18</sub> O <sub>49</sub> Nanowires as a New 980 nmâ€Laserâ€Driven Photothermal Agent for Efficient Ablation of Cancer Cells In Vivo. Advanced Materials, 2013, 25, 2095-2100.	21.0	370
5	Hierarchical mesoporous NiCo2O4@MnO2 core–shell nanowire arrays on nickel foam for aqueous asymmetric supercapacitors. Journal of Materials Chemistry A, 2014, 2, 4795.	10.3	355
6	Design and Functionalization of the NIR-Responsive Photothermal Semiconductor Nanomaterials for Cancer Theranostics. Accounts of Chemical Research, 2017, 50, 2529-2538.	15.6	312
7	Degradable Molybdenum Oxide Nanosheets with Rapid Clearance and Efficient Tumor Homing Capabilities as a Therapeutic Nanoplatform. Angewandte Chemie - International Edition, 2016, 55, 2122-2126.	13.8	254
8	Chain-like NiCo2O4 nanowires with different exposed reactive planes for high-performance supercapacitors. Journal of Materials Chemistry A, 2013, 1, 8560.	10.3	250
9	Cu7.2S4 nanocrystals: a novel photothermal agent with a 56.7% photothermal conversion efficiency for photothermal therapy of cancer cells. Nanoscale, 2014, 6, 3274.	5.6	239
10	Facile synthesis of biocompatible cysteine-coated CuS nanoparticles with high photothermal conversion efficiency for cancer therapy. Dalton Transactions, 2014, 43, 11709.	3.3	213
11	A Lowâ€Toxic Multifunctional Nanoplatform Based on Cu <sub>9</sub> S <sub>5</sub> @mSiO <sub>2</sub> Coreâ€Shell Nanocomposites: Combining Photothermal―and Chemotherapies with Infrared Thermal Imaging for Cancer Treatment. Advanced Functional Materials, 2013, 23, 4281-4292.	14.9	207
12	Highly aligned SnO2 nanorods on graphene sheets for gas sensors. Journal of Materials Chemistry, 2011, 21, 17360.	6.7	199
13	ZnO nanorods on reduced graphene sheets with excellent field emission, gas sensor and photocatalytic properties. Journal of Materials Chemistry A, 2013, 1, 8445.	10.3	193
14	High Detectivity Solarâ€Blind Highâ€Temperature Deepâ€Ultraviolet Photodetector Based on Multi‣ayered ( <i>l</i> 00) Facetâ€Oriented <i>l²</i> â€Ga <sub>2</sub> O <sub>3</sub> Nanobelts. Small, 2014, 10, 1848-1856	5. <sup>10.0</sup>	185
15	Design and synthesis of 3D interconnected mesoporous NiCo2O4@CoxNi1â^'x(OH)2 core–shell nanosheet arrays with large areal capacitance and high rate performance for supercapacitors. Journal of Materials Chemistry A, 2014, 2, 10090.	10.3	174
16	One pot synthesis of nickel foam supported self-assembly of NiWO <sub>4</sub> and CoWO <sub>4</sub> nanostructures that act as high performance electrochemical capacitor electrodes. Journal of Materials Chemistry A, 2015, 3, 14272-14278.	10.3	167
17	Hydrophilic Molybdenum Oxide Nanomaterials with Controlled Morphology and Strong Plasmonic Absorption for Photothermal Ablation of Cancer Cells. ACS Applied Materials & Interfaces, 2014, 6, 3915-3922.	8.0	166
18	Synthesis of hollow NiCo2O4 nanospheres with large specific surface area for asymmetric supercapacitors. Journal of Colloid and Interface Science, 2018, 511, 456-462.	9.4	163

#	Article	IF	CITATIONS
19	Three-dimensional-networked NiCo2S4 nanosheet array/carbon cloth anodes for high-performance lithium-ion batteries. NPG Asia Materials, 2015, 7, e195-e195.	7.9	158
20	Photothermal Theragnosis Synergistic Therapy Based on Bimetal Sulphide Nanocrystals Rather Than Nanocomposites. Advanced Materials, 2015, 27, 1339-1345.	21.0	149
21	Mechanism analysis of the capacitance contributions and ultralong cycling-stability of the isomorphous MnO <sub>2</sub> @MnO <sub>2</sub> core/shell nanostructures for supercapacitors. Journal of Materials Chemistry A, 2015, 3, 6168-6176.	10.3	138
22	A Dendritic Nickel Cobalt Sulfide Nanostructure for Alkaline Battery Electrodes. Advanced Functional Materials, 2018, 28, 1705937.	14.9	138
23	Solarâ€Inspired Water Purification Based on Emerging 2D Materials: Status and Challenges. Solar Rrl, 2020, 4, 1900400.	5.8	133
24	Facile synthesis of porous MnCo <sub>2</sub> O <sub>4.5</sub> hierarchical architectures for high-rate supercapacitors. CrystEngComm, 2014, 16, 2335-2339.	2.6	131
25	Hydrophilic Cu2ZnSnS4 nanocrystals for printing flexible, low-cost and environmentally friendly solar cells. CrystEngComm, 2012, 14, 3847.	2.6	125
26	Gold nanorods as a theranostic platform for in vitro and in vivo imaging and photothermal therapy of inflammatory macrophages. Nanoscale, 2015, 7, 13991-14001.	5.6	125
27	Epitaxial Heterostructures:Â Side-to-Side Siâ^'ZnS, Siâ^'ZnSe Biaxial Nanowires, and Sandwichlike ZnSâ^'Siâ^'ZnS Triaxial Nanowires. Journal of the American Chemical Society, 2003, 125, 11306-11313.	13.7	124
28	Tumor environment responsive degradable CuS@mSiO2@MnO2/DOX for MRI guided synergistic chemo-photothermal therapy and chemodynamic therapy. Chemical Engineering Journal, 2020, 389, 124450.	12.7	124
29	MnMoO <sub>4</sub> ·4H <sub>2</sub> O nanoplates grown on a Ni foam substrate for excellent electrochemical properties. Journal of Materials Chemistry A, 2014, 2, 20723-20728.	10.3	111
30	Effect of temperature on the performance of ultrafine MnO <sub>2</sub> nanobelt supercapacitors. Journal of Materials Chemistry A, 2014, 2, 1443-1447.	10.3	108
31	MnO2 ultralong nanowires with better electrical conductivity and enhanced supercapacitor performances. Journal of Materials Chemistry, 2012, 22, 14864.	6.7	101
32	Self-assembling hybrid NiO/Co3O4 ultrathin and mesoporous nanosheets into flower-like architectures for pseudocapacitance. Journal of Materials Chemistry A, 2013, 1, 9107.	10.3	101
33	Heterostructures of CuS nanoparticle/ZnO nanorod arrays on carbon fibers with improved visible and solar light photocatalytic properties. Journal of Materials Chemistry A, 2015, 3, 7304-7313.	10.3	95
34	Three-dimensional networked NiCo <sub>2</sub> O <sub>4</sub> /MnO <sub>2</sub> branched nanowire heterostructure arrays on nickel foam with enhanced supercapacitor performance. Journal of Materials Chemistry A, 2015, 3, 1717-1723.	10.3	94
35	Gallium Nitride Nanotubes by the Conversion of Gallium Oxide Nanotubes. Angewandte Chemie - International Edition, 2003, 42, 3493-3497.	13.8	93
36	Hierarchical hollow MnO2 nanofibers with enhanced supercapacitor performance. Journal of Colloid and Interface Science, 2018, 513, 448-454.	9.4	93

#	Article	IF	CITATIONS
37	Phase-controlled synthesis and gas-sensing properties of zinc stannate (ZnSnO3 and Zn2SnO4) faceted solid and hollow microcrystals. CrystEngComm, 2012, 14, 2172.	2.6	89
38	Folic acid-conjugated hollow mesoporous silica/CuS nanocomposites as a difunctional nanoplatform for targeted chemo-photothermal therapy of cancer cells. Journal of Materials Chemistry B, 2014, 2, 5358.	5.8	88
39	Bioinspired, Microstructured Silk Fibroin Adhesives for Flexible Skin Sensors. ACS Applied Materials & Interfaces, 2020, 12, 5601-5609.	8.0	83
40	Dendritic Heterojunction Nanowire Arrays for High-Performance Supercapacitors. Scientific Reports, 2015, 5, 7862.	3.3	82
41	In situ construction of heterostructured bimetallic sulfide/phosphide with rich interfaces for high-performance aqueous Zn-ion batteries. Science China Materials, 2022, 65, 356-363.	6.3	82
42	CuS@mSiO <sub>2</sub> -PEG core–shell nanoparticles as a NIR light responsive drug delivery nanoplatform for efficient chemo-photothermal therapy. Dalton Transactions, 2015, 44, 10343-10351.	3.3	80
43	Hydrophilic bismuth sulfur nanoflower superstructures with an improved photothermal efficiency for ablation of cancer cells. Nano Research, 2016, 9, 1934-1947.	10.4	80
44	Sn-Catalyzed Thermal Evaporation Synthesis of Tetrapod-Branched ZnSe Nanorod Architectures. Small, 2004, 1, 95-99.	10.0	79
45	Sn-Filled Single-Crystalline Wurtzite-Type ZnS Nanotubes. Angewandte Chemie - International Edition, 2004, 43, 4606-4609.	13.8	78
46	Cu <sub>2â^'x</sub> Se@mSiO <sub>2</sub> –PEG core–shell nanoparticles: a low-toxic and efficient difunctional nanoplatform for chemo-photothermal therapy under near infrared light radiation with a safe power density. Nanoscale, 2014, 6, 4361-4370.	5.6	77
47	Enhanced adsorption capacity of ultralong hydrogen titanate nanobelts for antibiotics. Journal of Materials Chemistry A, 2017, 5, 4352-4358.	10.3	76
48	Surface decoration of Bi2WO6 superstructures with Bi2O3 nanoparticles: an efficient method to improve visible-light-driven photocatalytic activity. CrystEngComm, 2013, 15, 9011.	2.6	75
49	A new strategy to effectively alleviate volume expansion and enhance the conductivity of hierarchical MnO@C nanocomposites for lithium ion batteries. Journal of Materials Chemistry A, 2017, 5, 21699-21708.	10.3	74
50	Self-assembled WO3â^'x hierarchical nanostructures for photothermal therapy with a 915 nm laser rather than the common 980 nm laser. Dalton Transactions, 2014, 43, 6244.	3.3	71
51	A self-powered broadband photodetector based on an n-Si(111)/p-NiO heterojunction with high photosensitivity and enhanced external quantum efficiency. Journal of Materials Chemistry C, 2017, 5, 12520-12528.	5.5	71
52	Macrophages-Mediated Delivery of Small Gold Nanorods for Tumor Hypoxia Photoacoustic Imaging and Enhanced Photothermal Therapy. ACS Applied Materials & Interfaces, 2019, 11, 15251-15261.	8.0	71
53	Oxygen vacancies-rich cobalt-doped NiMoO4 nanosheets for high energy density and stable aqueous Ni-Zn battery. Science China Materials, 2020, 63, 1205-1215.	6.3	71
54	Understanding the effect of polypyrrole and poly(3,4-ethylenedioxythiophene) on enhancing the supercapacitor performance of NiCo <sub>2</sub> O <sub>4</sub> electrodes. Journal of Materials Chemistry A, 2014, 2, 16731-16739.	10.3	70

#	Article	IF	CITATIONS
55	Sponge-like NiCo <sub>2</sub> O <sub>4</sub> /MnO <sub>2</sub> ultrathin nanoflakes for supercapacitor with high-rate performance and ultra-long cycle life. Journal of Materials Chemistry A, 2014, 2, 7738-7741.	10.3	69
56	"Transformed―Fe <sub>3</sub> S <sub>4</sub> tetragonal nanosheets: a high-efficiency and body-clearable agent for magnetic resonance imaging guided photothermal and chemodynamic synergistic therapy. Nanoscale, 2018, 10, 17902-17911.	5.6	69
5 <b>7</b>	Ni(OH) <sub>2</sub> /CoO/reduced graphene oxide composites with excellent electrochemical properties. Journal of Materials Chemistry A, 2013, 1, 478-481.	10.3	68
58	Carbon Nanotubes as Nanoreactors for Fabrication of Single-Crystalline Mg3N2Nanowires. Nano Letters, 2006, 6, 1136-1140.	9.1	67
59	A General Approach for the Growth of Metal Oxide Nanorod Arrays on Graphene Sheets and Their Applications. Chemistry - A European Journal, 2011, 17, 13912-13917.	3.3	66
60	Recent Progress of Methods to Enhance Photovoltaic Effect for Selfâ€Powered Heterojunction Photodetectors and Their Applications in Inorganic Lowâ€Dimensional Structures. Advanced Functional Materials, 2021, 31, 2011284.	14.9	66
61	An Interface Engineered Multicolor Photodetector Based on n‣i(111)/TiO <sub>2</sub> Nanorod Array Heterojunction. Advanced Functional Materials, 2016, 26, 1400-1410.	14.9	64
62	One-pot synthesis of large-scaled Janus Ag–Ag2S nanoparticles and their photocatalytic properties. CrystEngComm, 2011, 13, 7189.	2.6	62
63	Enhanced UV-visible light photodetectors with a TiO <sub>2</sub> /Si heterojunction using band engineering. Journal of Materials Chemistry C, 2017, 5, 12848-12856.	5.5	61
64	Novel semiconducting nanowire heterostructures: synthesis, properties and applications. Journal of Materials Chemistry, 2009, 19, 330-343.	6.7	59
65	Combined bortezomib-based chemotherapy and p53 gene therapy using hollow mesoporous silica nanospheres for p53 mutant non-small cell lung cancer treatment. Biomaterials Science, 2017, 5, 77-88.	5.4	59
66	Design and synthesis of 3D hierarchical NiCo <sub>2</sub> S <sub>4</sub> @MnO <sub>2</sub> core–shell nanosheet arrays for high-performance pseudocapacitors. RSC Advances, 2015, 5, 44642-44647.	3.6	57
67	Synthesis of hierarchical Co3O4@NiCo2O4 core-shell nanosheets as electrode materials for supercapacitor application. Journal of Alloys and Compounds, 2017, 700, 247-251.	5.5	57
68	Intracellular Mutual Amplification of Oxidative Stress and Inhibition Multidrug Resistance for Enhanced Sonodynamic/Chemodynamic/Chemo Therapy. Small, 2022, 18, e2107160.	10.0	57
69	Electrochemical Energy Storage Application and Degradation Analysis of Carbon-Coated Hierarchical NiCo2S4 Core-Shell Nanowire Arrays Grown Directly on Graphene/Nickel Foam. Scientific Reports, 2016, 6, 20264.	3.3	56
70	A Hybrid Electrode of Co3O4@PPy Core/Shell Nanosheet Arrays for High-Performance Supercapacitors. Nano-Micro Letters, 2016, 8, 143-150.	27.0	56
71	Fabrication of Metal-Semiconductor Nanowire Heterojunctions. Angewandte Chemie - International Edition, 2005, 44, 2140-2144.	13.8	52
72	Temperature-Dependent Growth of Germanium Oxide and Silicon Oxide Based Nanostructures, Aligned Silicon Oxide Nanowire Assemblies, and Silicon Oxide Microtubes. Small, 2005, 1, 429-438.	10.0	52

#	Article	IF	CITATIONS
73	Exceptional pseudocapacitive properties of hierarchical NiO ultrafine nanowires grown on mesoporous NiO nanosheets. Journal of Materials Chemistry A, 2014, 2, 12799-12804.	10.3	52
74	Ta3N5-Pt nonwoven cloth with hierarchical nanopores as efficient and easily recyclable macroscale photocatalysts. Scientific Reports, 2014, 4, 3978.	3.3	52
75	Degradable rhenium trioxide nanocubes with high localized surface plasmon resonance absorbance like gold for photothermal theranostics. Biomaterials, 2018, 159, 68-81.	11.4	52
76	A novel and facile synthesis of porous SiO <sub>2</sub> -coated ultrasmall Se particles as a drug delivery nanoplatform for efficient synergistic treatment of cancer cells. Nanoscale, 2016, 8, 8536-8541.	5.6	50
77	Probing the intermolecular interaction mechanisms between humic acid and different substrates with implications for its adsorption and removal in water treatment. Water Research, 2020, 176, 115766.	11.3	50
78	Surface disorder engineering in ZnCdS for cocatalyst free visible light driven hydrogen production. Nano Research, 2022, 15, 996-1002.	10.4	50
79	One-pot morphology-controlled synthesis of various shaped mesoporous silica nanoparticles. Journal of Materials Science, 2013, 48, 5718-5726.	3.7	49
80	Surface Coating Constraint Induced Anisotropic Swelling of Silicon in Si–Void@SiO <i><sub>x</sub></i> Nanowire Anode for Lithiumâ€lon Batteries. Small, 2017, 13, 1603754.	10.0	49
81	MnO <sub>2</sub> Nanoflower Arrays with High Rate Capability for Flexible Supercapacitors. ChemElectroChem, 2014, 1, 1003-1008.	3.4	48
82	Nanoparticles Encapsulated in Porous Carbon Matrix Coated on Carbon Fibers: An Ultrastable Cathode for Liâ€ion Batteries. Advanced Energy Materials, 2017, 7, 1601363.	19.5	48
83	Lightly doped single crystalline porous Si nanowires with improved optical and electrical properties. Journal of Materials Chemistry, 2011, 21, 801-805.	6.7	47
84	CuCo <sub>2</sub> S <sub>4</sub> nanocrystals: a new platform for multimodal imaging guided photothermal therapy. Nanoscale, 2017, 9, 2626-2632.	5.6	47
85	CoMoO <sub>4</sub> ·0.9H <sub>2</sub> O nanorods grown on reduced graphene oxide as advanced electrochemical pseudocapacitor materials. RSC Advances, 2014, 4, 34307.	3.6	46
86	Right Cu <sub>2â^'</sub> <i><sub>x</sub></i> S@MnS Core–Shell Nanoparticles as a Photo/H <sub>2</sub> O <sub>2</sub> â€Responsive Platform for Effective Cancer Theranostics. Advanced Science, 2019, 6, 1901461.	11.2	45
87	Carbon-coated mesoporous NiO nanoparticles as an electrode material for high performance electrochemical capacitors. New Journal of Chemistry, 2013, 37, 4031.	2.8	44
88	Hydrous RuO <sub>2</sub> nanoparticles as an efficient NIR-light induced photothermal agent for ablation of cancer cells in vitro and in vivo. Nanoscale, 2015, 7, 11962-11970.	5.6	44
89	Facile synthesis of 3D flower-like porous NiO architectures with an excellent capacitance performance. RSC Advances, 2015, 5, 47506-47510.	3.6	42
90	NaYF <sub>4</sub> :Yb/Er@PPy core–shell nanoplates: an imaging-guided multimodal platform for photothermal therapy of cancers. Nanoscale, 2016, 8, 1040-1048.	5.6	42

#	Article	IF	CITATIONS
91	Arbitrary Multicolor Photodetection by Hetero-integrated Semiconductor Nanostructures. Scientific Reports, 2013, 3, 2368.	3.3	41
92	Synthesis and Field-Emission Properties of Ga2O3â^'C Nanocables. Chemistry of Materials, 2004, 16, 5158-5161.	6.7	40
93	Controllable hydrothermal synthesis, growth mechanism, and properties of ZnO three-dimensional structures. New Journal of Chemistry, 2010, 34, 732.	2.8	39
94	Cobalt nickel nitride coated by a thin carbon layer anchoring on nitrogen-doped carbon nanotube anodes for high-performance lithium-ion batteries. Journal of Materials Chemistry A, 2018, 6, 19853-19862.	10.3	38
95	A simple transformation from silica core–shell–shell to yolk–shell nanostructures: a useful platform for effective cell imaging and drug delivery. Journal of Materials Chemistry, 2012, 22, 17011.	6.7	37
96	CuCo <sub>2</sub> S <sub>4</sub> nanocrystals as a nanoplatform for photothermal therapy of arterial inflammation. Nanoscale, 2019, 11, 9733-9742.	5.6	37
97	A full-spectrum-absorption from nickel sulphide nanoparticles for efficient NIR-II window photothermal therapy. Nanoscale, 2019, 11, 20161-20170.	5.6	37
98	Highly ordered mesoporous NiCo <sub>2</sub> O <sub>4</sub> with superior pseudocapacitance performance for supercapacitors. Journal of Materials Chemistry A, 2015, 3, 11503-11510.	10.3	36
99	Hollow Co3O4@MnO2 Cubic Derived From ZIF-67@Mn-ZIF as Electrode Materials for Supercapacitors. Frontiers in Chemistry, 2019, 7, 831.	3.6	35
100	Biodegradable hollow manganese/cobalt oxide nanoparticles for tumor theranostics. Nanoscale, 2019, 11, 23021-23026.	5.6	35
101	Unconventional Ribbon-Shaped β-Ga <sub>2</sub> O <sub>3</sub> Tubes with Mobile Sn Nanowire Fillings. ACS Nano, 2008, 2, 107-112.	14.6	34
102	Polypyrrole-encapsulated iron tungstate nanocomposites: a versatile platform for multimodal tumor imaging and photothermal therapy. Nanoscale, 2016, 8, 12917-12928.	5.6	34
103	A Novel Photothermal Nanocrystals of Cu7S4 Hollow Structure for Efficient Ablation of Cancer Cells. Nano-Micro Letters, 2014, 6, 169-177.	27.0	33
104	Tumor Microenvironment Responsive Biodegradable Feâ€Doped MoO <i><sub>x</sub></i> Nanowires for Magnetic Resonance Imaging Guided Photothermalâ€Enhanced Chemodynamic Synergistic Antitumor Therapy. Advanced Healthcare Materials, 2021, 10, e2001665.	7.6	33
105	Morphology-selective synthesis and wettability properties of well-aligned Cu2-xSe nanostructures on a copper substrate. Journal of Materials Chemistry, 2011, 21, 3053.	6.7	32
106	In situ preparation of CuInS2 films on a flexible copper foil and their application in thin film solar cells. CrystEngComm, 2012, 14, 1825.	2.6	32
107	Facile synthesis of hydrophilic polypyrrole nanoparticles for photothermal cancer therapy. Journal of Materials Science, 2014, 49, 3484-3490.	3.7	32
108	Hierarchical multicomponent electrode with NiMoO4 nanosheets coated on Co3O4 nanowire arrays for enhanced electrochemical properties. Journal of Alloys and Compounds, 2019, 781, 1127-1131.	5.5	32

#	Article	IF	CITATIONS
109	An effective approach to reduce inflammation and stenosis in carotid artery: polypyrrole nanoparticle-based photothermal therapy. Nanoscale, 2015, 7, 7682-7691.	5.6	30
110	Hierarchical core/shell structures of ZnO nanorod@CoMoO <sub>4</sub> nanoplates used as a high-performance electrode for supercapacitors. RSC Advances, 2016, 6, 3020-3024.	3.6	30
111	Heterostructures of vertical, aligned and dense SnO2 nanorods on graphene sheets: in situ TEM measured mechanical, electrical and field emission properties. Journal of Materials Chemistry, 2012, 22, 19196.	6.7	29
112	NiCo <sub>2</sub> O <sub>4</sub> Nanostructures as a Promising Alternative for NiO Photocathodes in pâ€Type Dyeâ€Sensitized Solar Cells with High Efficiency. Energy Technology, 2014, 2, 517-521.	3.8	29
113	Stabilizing Lithium–Sulfur Batteries through Control of Sulfur Aggregation and Polysulfide Dissolution. Small, 2018, 14, e1703816.	10.0	28
114	Porous cobalt sulfide hollow nanospheres with tunable optical property for magnetic resonance imaging-guided photothermal therapy. Nanoscale, 2018, 10, 14190-14200.	5.6	28
115	Magnetic-field-assisted hydrothermal synthesis of 2 × 2 tunnels of MnO <sub>2</sub> nanostructures with enhanced supercapacitor performance. CrystEngComm, 2014, 16, 9987-9991.	2.6	27
116	Na <sub>0.3</sub> WO <sub>3</sub> nanorods: a multifunctional agent for in vivo dual-model imaging and photothermal therapy of cancer cells. Dalton Transactions, 2015, 44, 2771-2779.	3.3	27
117	Growth of TiO <sub>2</sub> nanorod bundles on carbon fibers as flexible and weaveable photocatalyst/photoelectrode. RSC Advances, 2015, 5, 102868-102876.	3.6	27
118	SnS nanosheets for efficient photothermal therapy. New Journal of Chemistry, 2016, 40, 4464-4467.	2.8	27
119	In situ transmission electron microscopy study of individual nanostructures during lithiation and delithiation processes. Journal of Materials Chemistry A, 2017, 5, 20072-20094.	10.3	27
120	Prospective important semiconducting nanotubes: synthesis, properties and applications. Journal of Materials Chemistry, 2009, 19, 7592.	6.7	26
121	PEG-mediated solvothermal synthesis of NaYF4:Yb/Er superstructures with efficient upconversion luminescence. Journal of Alloys and Compounds, 2010, 506, L17-L21.	5.5	26
122	Construction of 980 nm laser-driven dye-sensitized photovoltaic cell with excellent performance for powering nanobiodevices implanted under the skin. Journal of Materials Chemistry, 2012, 22, 18156.	6.7	26
123	Synthesis of CuS nanoplate-containing PDMS film with excellent near-infrared shielding properties. RSC Advances, 2016, 6, 18881-18890.	3.6	26
124	Treatment of steroid-induced osteonecrosis of the femoral head using porous Se@SiO2 nanocomposites to suppress reactive oxygen species. Scientific Reports, 2017, 7, 43914.	3.3	25
125	Hierarchical assembly of manganese dioxide nanosheets on one-dimensional titanium nitride nanofibers for high-performance supercapacitors. Journal of Colloid and Interface Science, 2019, 552, 712-718.	9.4	25
126	Recent Research on One-Dimensional Silicon-Based Semiconductor Nanomaterials: Synthesis, Structures, Properties and Applications. Critical Reviews in Solid State and Materials Sciences, 2011, 36, 148-173.	12.3	24

#	Article	IF	CITATIONS
127	"All-in-One―Theranostic Agent with Seven Functions Based on Bi-Doped Metal Chalcogenide Nanoflowers. ACS Applied Materials & Interfaces, 2019, 11, 45467-45478.	8.0	24
128	Nanofabrication on ZnO nanowires. Applied Physics Letters, 2006, 89, 243111.	3.3	23
129	SnO2 nanoribbons: excellent field-emitters. CrystEngComm, 2011, 13, 2289.	2.6	23
130	Melting of Metallic Electrodes and Their Flowing Through a Carbon Nanotube Channel within a Device. Advanced Materials, 2013, 25, 2693-2699.	21.0	23
131	An easy-to-fabricate clearable CuS-superstructure-based multifunctional theranostic platform for efficient imaging guided chemo-photothermal therapy. Nanoscale, 2018, 10, 11430-11440.	5.6	23
132	Reversible formation of networked porous Sb nanoparticles during cycling: Sb nanoparticles encapsulated in a nitrogen-doped carbon matrix with nanorod structures for high-performance Li-ion batteries. Journal of Materials Chemistry A, 2019, 7, 24292-24300.	10.3	23
133	New Strategy for Specific Eradication of Implant-Related Infections Based on Special and Selective Degradability of Rhenium Trioxide Nanocubes. ACS Applied Materials & amp; Interfaces, 2019, 11, 25691-25701.	8.0	21
134	UV and visible light synergetic photodegradation using rutile TiO <sub>2</sub> nanorod arrays based on a p–n Junction. Dalton Transactions, 2017, 46, 4296-4302.	3.3	19
135	A facile method to fabricated UV–Vis photodetectors based on TiO2/Si heterojunction. Applied Surface Science, 2018, 449, 358-362.	6.1	19
136	Tumor microenvironment responsive self-cascade catalysis for synergistic chemo/chemodynamic therapy by multifunctional biomimetic nanozymes. Journal of Materials Chemistry B, 2022, 10, 637-645.	5.8	18
137	Hydrothermal control growth of Zn2GeO4–diethylenetriamine 3D dumbbell-like nanobundles. CrystEngComm, 2014, 16, 3222.	2.6	17
138	An efficiently enhanced UV-visible light photodetector with a Zn:NiO/p-Si isotype heterojunction. Journal of Materials Chemistry C, 2020, 8, 3498-3508.	5.5	17
139	Hydrothermal synthesis, growth mechanism, and properties of three-dimensional micro/nanoscaled hierarchical architecture films of hemimorphite zinc silicate. CrystEngComm, 2011, 13, 2273.	2.6	16
140	Large-scale, uniform, single-crystalline Cd(OH)2 hexagonal platelets for Cd-based functional applications. CrystEngComm, 2010, 12, 1726.	2.6	15
141	Molten Au/Ge Alloy Migration in Ge Nanowires. Nano Letters, 2015, 15, 2809-2816.	9.1	15
142	Janus Ag/Ag <sub>2</sub> S beads as efficient photothermal agents for the eradication of inflammation and artery stenosis. Nanoscale, 2019, 11, 20324-20332.	5.6	15
143	Controllable Hydrothermal Synthesis and Photocatalytic Performance of Bi2MoO6 Nano/Microstructures. Catalysts, 2020, 10, 1161.	3.5	15
144	AgFeS <sub>2</sub> nanoparticles as a novel photothermal platform for effective artery stenosis therapy. Nanoscale, 2020, 12, 11288-11296.	5.6	15

#	Article	IF	CITATIONS
145	A controllable hydrothermal synthesis of uniform three-dimensional hierarchical microstructured ZnO films. CrystEngComm, 2011, 13, 6107.	2.6	14
146	Synthesis strategies and biomedical applications for doped inorganic semiconductor nanocrystals. Cell Reports Physical Science, 2021, 2, 100436.	5.6	14
147	Programmable DNA Framework Sensors for In Situ Cell-Surface pH Analysis. Analytical Chemistry, 2021, 93, 12170-12174.	6.5	14
148	Liquid Gallium Columns Sheathed with Carbon:  Bulk Synthesis and Manipulation. Journal of Physical Chemistry B, 2005, 109, 11580-11584.	2.6	13
149	New nanowire heterostructures: SnO <sub>2</sub> nanowires epitaxial growth on Si bicrystalline nanowires. CrystEngComm, 2010, 12, 89-93.	2.6	13
150	In situ transmission electron microscope studies on one-dimensional nanomaterials: Manipulation, properties and applications. Progress in Materials Science, 2020, 113, 100674.	32.8	13
151	Recent developments of infrared photodetectors with low-dimensional inorganic nanostructures. Nano Research, 2022, 15, 805-817.	10.4	13
152	Rapid Fabrication of Nanocrystals through in situ Electron Beam Irradiation in a Transmission Electron Microscope. Journal of Physical Chemistry C, 2009, 113, 5201-5205.	3.1	12
153	Rectangular or square, tapered, and single-crystal PbTe nanotubes. Journal of Materials Chemistry, 2009, 19, 3063.	6.7	12
154	ZnO–Si side-to-side biaxial nanowire heterostructures with improved luminescence. Journal of Materials Chemistry, 2009, 19, 7011.	6.7	12
155	Ethanol gas sensor based on a self-supporting hierarchical SnO <sub>2</sub> nanorods array. CrystEngComm, 2015, 17, 1800-1804.	2.6	12
156	Degradable Molybdenum Oxide Nanosheets with Rapid Clearance and Efficient Tumor Homing Capabilities as a Therapeutic Nanoplatform. Angewandte Chemie, 2016, 128, 2162-2166.	2.0	12
157	Engineering DNA quadruplexes in DNA nanostructures for biosensor construction. Nano Research, 2022, 15, 3504-3513.	10.4	12
158	Flower-like Fe <sub>7</sub> S <sub>8</sub> /Bi <sub>2</sub> S <sub>3</sub> superstructures with improved near-infrared absorption for efficient chemo-photothermal therapy. Dalton Transactions, 2019, 48, 3360-3368.	3.3	11
159	High-efficiency and safe sulfur-doped iron oxides for magnetic resonance imaging-guided photothermal/magnetic hyperthermia therapy. Dalton Transactions, 2020, 49, 5493-5502.	3.3	11
160	A Mobile Sn Nanowire Inside a <i>βâ€</i> Ga <sub>2</sub> O <sub>3</sub> Tube: A Practical Nanoscale Electrically/Thermally Driven Switch. Small, 2011, 7, 3377-3384.	10.0	10
161	Highly Ordered Mesoporous NiCo2O4 as a High Performance Anode Material for Li-Ion Batteries. Frontiers in Chemistry, 2019, 7, 521.	3.6	10
162	Uniform ZnSe microspheres self-assembled from ZnSe polyhedron shaped nanocrystals. CrystEngComm, 2011, 13, 1518-1524.	2.6	9

#	Article	IF	CITATIONS
163	Synthesis of Cu <sub>2</sub> ZnSnS <sub>4</sub> film by air-stable molecular-precursor ink for constructing thin film solar cells. RSC Advances, 2014, 4, 36046.	3.6	9
164	Hydrophilic K <sub>2</sub> Mn <sub>4</sub> O <sub>8</sub> nanoflowers as a sensitive photothermal theragnosis synergistic platform for the ablation of cancer. New Journal of Chemistry, 2018, 42, 3714-3721.	2.8	9
165	An adjustable multi-color detector based on regulating TiO2 surface adsorption and multi-junction synergy. Nano Research, 2021, 14, 3423-3430.	10.4	9
166	In situ structural evolution from GeO nanospheres to GeO/(Ge, GeO2) core-shell nanospheres and to Ge hollow nanospheres. CrystEngComm, 2011, 13, 4611.	2.6	8
167	Nanocomposites: A Low-Toxic Multifunctional Nanoplatform Based on Cu9S5@mSiO2Core-Shell Nanocomposites: Combining Photothermal- and Chemotherapies with Infrared Thermal Imaging for Cancer Treatment (Adv. Funct. Mater. 35/2013). Advanced Functional Materials, 2013, 23, 4280-4280.	14.9	8
168	A high performance self-powered heterojunction photodetector based on NiO nanosheets on an n-Si (1 0 0) modified substrate. Materials Letters, 2021, 285, 128995.	2.6	8
169	Uniform, thin and continuous graphitic carbon tubular coatings on CdS nanowires. Journal of Materials Chemistry, 2009, 19, 1093.	6.7	7
170	Single-crystal MgS nanotubes: synthesis and properties. CrystEngComm, 2010, 12, 1286-1289.	2.6	7
171	Hierarchical architectures of Co <sub>3</sub> O <sub>4</sub> ultrafine nanowires grown on Co <sub>3</sub> O <sub>4</sub> nanowires with fascinating electrochemical performance. New Journal of Chemistry, 2016, 40, 377-384.	2.8	7
172	Battery Electrodes: A Dendritic Nickel Cobalt Sulfide Nanostructure for Alkaline Battery Electrodes (Adv. Funct. Mater. 23/2018). Advanced Functional Materials, 2018, 28, 1870154.	14.9	7
173	Excellent Field Emitters: Onion-Shaped Tipped Carbon Nanotubes. Journal of Physical Chemistry C, 2010, 114, 8282-8286.	3.1	6
174	A facile approach for the synthesis of Cu2â^'x Se nanowires and their field emission properties. Journal of Materials Science, 2014, 49, 532-537.	3.7	6
175	Facile synthesis of graphene nanoribbons from zeolite-templated ultra-small carbon nanotubes for lithium ion storage. Journal of Materials Chemistry A, 2018, 6, 21327-21334.	10.3	6
176	Fast Modulation of Surface Amphiphobicity/Amphiphilicity via Bidirectional Substitution between Perfluorinated Surfactants and Polyanions throughout Pre-Assembled Polyelectrolyte Multilayers. Langmuir, 2019, 35, 17122-17131.	3.5	6
177	High-precision, large-domain three-dimensional manipulation of nano-materials for fabrication nanodevices. Nanoscale Research Letters, 2011, 6, 473.	5.7	5
178	A simple method for preparing a TiO <sub>2</sub> -based back-gate controlled N-channel MSM–IGFET UV photodetector. Journal of Materials Chemistry C, 2020, 8, 1781-1787.	5.5	5
179	NixCo3â^'xS4@NiCo2O4 hybrid composites as supercapacitors electrode material. Materials Letters, 2017, 191, 101-104.	2.6	4
180	Large scaled hexagonal prismatic sub-micro sized Mg crystals by a vapor–liquid–solid process. Chemical Communications, 2009, , 4503.	4.1	3

#	Article	IF	CITATIONS
181	Cover Picture: MnO2 Nanoflower Arrays with High Rate Capability for Flexible Supercapacitors		